Journal of Applied Physics

Surface effects and magnetic ordering in few-nanometer-sized ε-Fe_2O_3 particles

Cite as: J. Appl. Phys. **114**, 163911 (2013); https://doi.org/10.1063/1.4827839
Submitted: 30 September 2013 . Accepted: 14 October 2013 . Published Online: 30 October 2013

D. A. Balaev, A. A. Dubrovskiy, K. A. Shaykhutdinov, O. A. Bayukov, S. S. Yakushkin, G. A. Bukhtiyarova, and O. N. Martyanov

Surface effects and magnetic ordering in few-nanometer-sized ε-Fe_2O_3 particles

D. A. Balaev,[1] A. A. Dubrovskiy,[1] K. A. Shaykhutdinov,[1] O. A. Bayukov,[1] S. S. Yakushkin,[2] G. A. Bukhtiyarova,[2] and O. N. Martyanov[2]
[1]*Kirensky Institute of Physics, Russian Academy of Sciences, Siberian Branch, Krasnoyarsk 660036, Russia*
[2]*Boreskov Institute of Catalysis, Russian Academy of Sciences, Siberian Branch, Novosibirsk 630090, Russia*

(Received 30 September 2013; accepted 14 October 2013; published online 30 October 2013)

The magnetic properties of ε-Fe_2O_3 nanoparticles with an average size of 3.4 nm in a silica gel matrix are investigated using Mössbauer technique, electron spin resonance, and magnetic measurements. Two magnetic subsystems reveal in magnetic measurements. Paramagnetic subsystem is formed by the Fe(III) ions in the smallest (<3.5 nm) particles' shell, while ferrimagnetic ordering in the "core" of the particles results in superparamagnetic behavior. The superparamagnetic behavior of the investigated samples is observed up to ~800 K. The magnetic moment of the particles is formed by both the ferrimagnetic ordering characteristic of ε-Fe_2O_3 and the additional effect of uncompensated sublattices (planes). © *2013 AIP Publishing LLC*. [http://dx.doi.org/10.1063/1.4827839]

I. INTRODUCTION

Modification of the magnetic properties of magnetically ordered particles with a decrease in their size down to few nanometers evokes intensive studies in this direction. The effects observed in such particles are related, as a rule, to the growing fraction of surface atoms, which offers opportunities for new applications of magnetic nanoparticles and facilitates a deeper understanding of physics of magnetically ordered systems on such a small scale.

Numerous studies of ferro-, ferri-, and antiferromagnetic nanoparticles demonstrate a significant difference of their magnetic properties from those of bulk materials. In particular, antiferromagnetic oxide nanoparticles exhibit a considerable magnetic moment formed by uncompensated magnetically active atoms or planes.[1] In ferro- and ferrimagnetically ordered oxide particles, the saturation magnetization appears, as a rule, lower than in bulk materials, which can be caused by broken bonds and disordered magnetic moments of surface atoms. The temperature of the transition to the magnetically ordered state usually decreases with an increase in the particle size (see, for example, Refs. 1–5), although in MnO nanoparticles, the Neel temperature growth was observed.[6,7]

Among structural modifications of trivalent Fe(III) iron oxide, α- and γ-Fe_2O_3 nanoparticles are best investigated.[1–3,8–13] The ε-Fe_2O_3 polymorphic modification was reliably identified for the first time in 1998.[14] The structure of this phase is intermediate between the structures of α and γ modifications of Fe(III) iron oxide (One more Fe_2O_3 modification, β-Fe_2O_3, is also a fairly rare iron oxide polymorph[15]). Due to its low surface energy, the ε-Fe_2O_3 phase exists in the form of particles 25–100 nm in size,[15] so most of the available data were obtained on such particles.[16–26] In the ε-Fe_2O_3 crystal structure, iron atoms occupy four nonequivalent positions and the competition of the exchange interactions of Fe^{3+} atoms in different planes leads to the ferrimagnetic ordering.[16,21,22] Mössbauer spectroscopy, neutron diffraction, and magnetostatic measurement data showed that ε-Fe_2O_3 can be considered as a canted ferrimagnet.[16–22] The authors of study[22] attributed the magnetic transition observed at $T \sim 110$ K to the change in the sublattice canting angle (analogously to the Morin point in a weak ferromagnet). Another possible cause of this transition is the formation of a square-wave structure at this temperature.[23] At room temperature, the magnetization curves show the large coercivity ($H_C \sim 20$ kOe) and the temperature of the transition from the paramagnetic to magnetically ordered state, according to the data reported in Refs. 16, 18, 20–22, 25, and 26, lies within 500–585 K.

The ε-Fe_2O_3 phase is metastable and, as the particle size is increased, transforms to the α-Fe_2O_3 phase. At the same time, a decrease in the oxide phase size during synthesis can lead to the formation of γ-Fe_2O_3. The authors of study[27] showed that, varying the average nanoparticle size, one can change the phase composition of oxide nanoparticles. It was demonstrated that the ε-Fe_2O_3 phase cannot exist in the form of free, not deposited on a substrate, nanoparticles with a size less than 8 nm.

In recent studies,[28,29] the technique for fabricating ε-Fe_2O_3 in a silica gel matrix was reported, which allows obtaining particles with an average size of few nanometers. The results of the magnetostatic and electron spin resonance (ESR) studies of the particles with a size from 2 to 15 nm were reported in Ref. 30. At these sizes, which are much smaller than 25÷100 nm,[16–26] the magnetically ordered particles exhibit the superparamagnetic (SP) behavior. Here, we investigate the ε-Fe_2O_3 particles with a characteristic size of no more than 6 nm. We focus upon the role of surface atoms in the formation of the magnetic moment of such particles.

II. EXPERIMENTAL

We synthesized ε-Fe_2O_3 samples with different Fe(III) weight contents in a porous silica gel matrix by incipient wetness impregnation with Fe(II) sulfates[28,29] and subsequent drying at $T = 110$ °C and calcination at temperatures

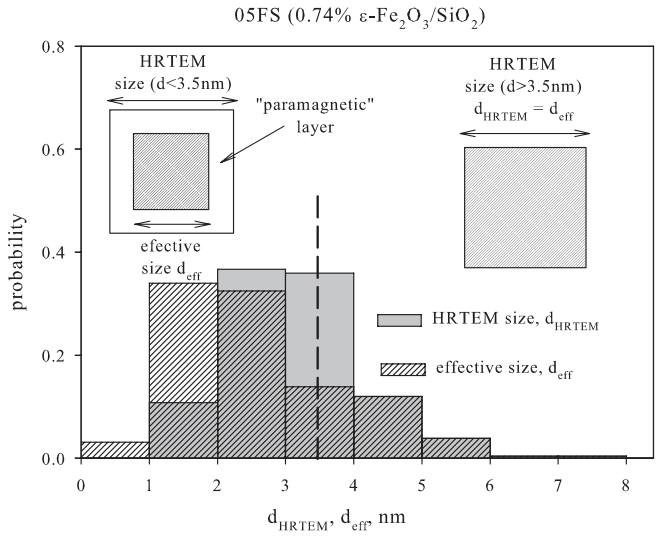

FIG. 1. Size (d_{HRTEM}) distribution of ε-Fe_2O_3 particles in sample 05FS (0.74% ε-Fe_2O_3/SiO_2) obtained from the HRTEM data and effective size ($d_{eff} = d_{HRTEM} - 2 \times 0.31$ nm) distribution with regard to "paramagnetic" surface Fe(III) atoms for $d_{HRTEM} < 3.5$ nm (shown by the vertical dashed line). Schematic of the model for the particles with $d_{HRTEM} < 3.5$ nm and $d_{HRTEM} > 3.5$ nm.

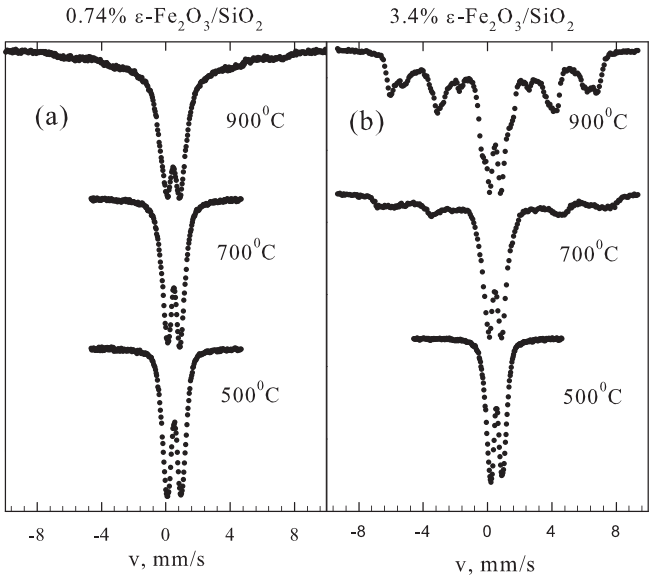

FIG. 2. Mössbauer spectra of the samples with (a) 0.74% (05FS) and (b) 3.4% Fe (3FS) annealed at different temperatures.

of 400–900 °C for 4 h. The ε-Fe_2O_3/SiO_2 samples with the Fe(III) contents of about 0.74 and 3.4 wt. %, hereinafter denoted as 05FS and 3FS, were investigated; sample 3FS was used as a reference for comparing the Mössbauer spectra.

According to the data of high resolution transmission electron microscopy (HRTEM) with the use of a JEOL JEM-2010 microscope (resolution 1.4 Å, accelerating voltage 200 kV), the sample consists mainly of particles with the size $d = 1.3 \div 6$ nm (Fig. 1); the amount of particles $6 \div 8$ nm in size was less than 1%. In the presented microscopic images, the measured interplanar distances in particles correspond to the ε-Fe_2O_3 phase.[30]

Mössbauer spectra were recorded at room temperature using a conventional spectrometer equipped with a ^{57}Co(Cr) source.

The magnetic properties were studied on a vibrating sample magnetometer in the temperature range of 4.2–300 K. The experimental data on magnetization are given in emu divided by a Fe_2O_3 mass in the sample. Magnetization was measured in the temperature range of 300–1000 K on a PPMS-6000 facility (Quantum Design) on the powder sample glued onto the substrate and placed in high vacuum with a residual pressure of $\sim 10^{-10}$ Torr.

The electron spin resonance spectra were recorded with a Bruker ELEXSYS 500 X-band ESR spectrometer. The samples were placed at the center of a high-temperature rectangular TE102 cavity. For measurements, at temperatures up to 800 K, the sample was exhausted to obtain the identical conditions of the high-temperature magnetostatic and magnetic resonance measurements.

III. RESULTS AND DISCUSSION

The final stage of the samples' synthesis is annealing in air.[28,29] At temperatures above 600 °C, the ε-Fe_2O_3 phase forms; at T = 900 °C, its content is maximum and no impurities of other Fe_2O_3 polymorphs are observed.[29] Figure 2 shows the Mössbauer spectra for samples 05FS and 3FS calcined at different temperatures.

It can be seen from Fig. 2(b) that with increasing annealing temperature, a magnetically ordered phase identified by Zeeman sextets in the spectrum is formed in 3FS. The sextet parameters of the sample with a Fe content of 3.4% after annealing at 900 °C correspond to the octahedral and tetrahedral positions of the phase,[16] which indicates the formation of ε-Fe_2O_3 particles. No other iron oxide phases are observed in the sample. In sample 05FS (Fig. 2(a)), large ε-Fe_2O_3 particles do not form due to the spatial stabilization, which limits the mass transfer during crystallization.

The superparamagnetic behavior of the investigated ε-Fe_2O_3 nanoparticles manifests itself in the blocking temperature revealed from the temperature dependences of the magnetic moment M(T) in the field (FC) and zero field cooling (ZFC) regimes presented in Fig. 3. The dependence ZFC M(T) at H = 1 kOe has a pronounced maximum; for the FC regime, there is no maxima. For these two regimes, the M(T) data at H = 1 kOe diverge at a temperature of about 35 K (inset in Fig. 3). At H = 10 kOe, the dependences M(T) coincide up to $T \approx 4.5$ K; the magnetic moment monotonically grows with decreasing temperature. The analogous considerable growth of the M(T) values with decreasing temperature is observed at H = 60 kOe.

The dependence M(H) at T = 4.2 K is irreversible in field range up to ~20 kOe, which is characteristic of SP system below the blocking temperature. Additionally, the M(H) growth is observed for higher fields (Fig. 4). Such a behavior of the magnetization curves is typical of systems with paramagnetic ions.

Thus, magnetic measurements reveal contributions of SP and paramagnetic subsystems. The contribution of SP subsystem is usually simulated by the Langevin function. For the magnetic moment of SP particles of hundreds Bohr

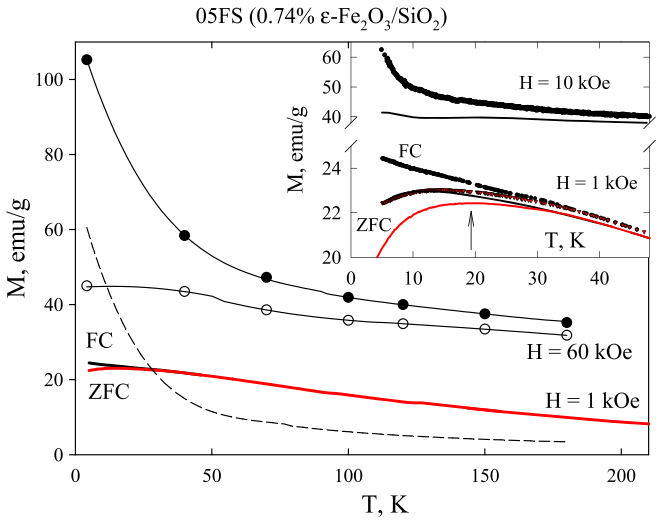

FIG. 3. Experimental temperature dependences M(H = 60 kOe) (dark symbols) for the investigated sample and SP contribution at H = 60 kOe (light symbols) after subtraction of the paramagnetic contribution 65 emu/g × B(H, T) (dashed curve). Temperature dependences of the magnetic moment M(T) in the ZFC and FC regimes. Inset: M(T) in the fields H = 1 (ZFC and FC) and 10 kOe (symbols) and corresponding SP contributions (solid curves). The arrow shows the blocking temperature at H = 1 kOe.

magnetons (see below), the Langevin function L(H, T) at temperatures below 100 K in the field H ~ 60 kOe is close to saturation (L(H, T) ≈ 1). In this case, comparison of the magnetization curves obtained at different temperatures and the dependences M(T) obtained in different fields made it possible to determine the contribution of the paramagnetic phase in the magnetic moment of the sample. This contribution amounts to 65 ± 5 (emu/g) × B(H, T), where B(H, T) is the Brillouin function with the spin S = 5/2 and g-factor equals to 2 for an Fe(III) atom. For the cubic shape approximation and particle size distribution (Fig. 1), the value 65 emu/g corresponds to ≈50% of total surface of the particles (and ≈19% of total amount of Fe(III) atoms). For 3FS sample having sufficiently wider particle size distribution (up to 15 nm)[29,30] similar approach gives substantially smaller contribution of paramagnetic phase (13 ± 2 emu/g × B(H, T) which corresponds to ≈18% of total surface of the particles and ≈3.7% of total amount of Fe(III) atoms). So, the existence of paramagnetic contribution is attributed to the smallest particles.

The data obtained by subtracting the paramagnetic contribution are presented in Fig. 4. It can be seen that the dependence M(H) is typical of a system of SP particles below blocking temperature T_B, which amounts to ~20 K at H = 1 kOe.

It is reasonably to assume that Fe(III) atoms on the surface of the smallest particles are responsible for the paramagnetic contribution discussed. According to HRTEM data and obtained values of paramagnetic contribution, it is possible to estimate the characteristic size of the particles in which the surface Fe(III) atoms are paramagnetic. In the assumption of a cubic shape of the particles, this size is about 3.5 ± 0.3 nm both for 05FS and 3FS samples (in the estimation, an average distance of 3.1 Å between Fe atoms was taken[21]). The paramagnetic behavior of surface spins is most likely caused by unsaturated chemical bonds of the surface iron atoms, which was previously observed for small oxide particles.[12,31,32] Note that no noticeable anomalies in the magnetic properties that would evidence the freezing effects or surface spin pinning[10–13,32] were observed in the samples under study.

Thus, for the particles with the characteristic size below ~3.5 nm, the paramagnetic behavior of the surface atoms is observed. Atoms of the inner layers are involved in the magnetic structure formation. In the first approximation, the interaction of the core and the surface in such particles can be ignored. In this case, atoms of inner layers can be considered as a SP particle with the effective size $d_{eff} = d - 2 \times 0.31$ nm. The schematic of this model and the distribution of particles over the effective size, i.e., the size of a magnetically ordered core are presented in Fig. 1.

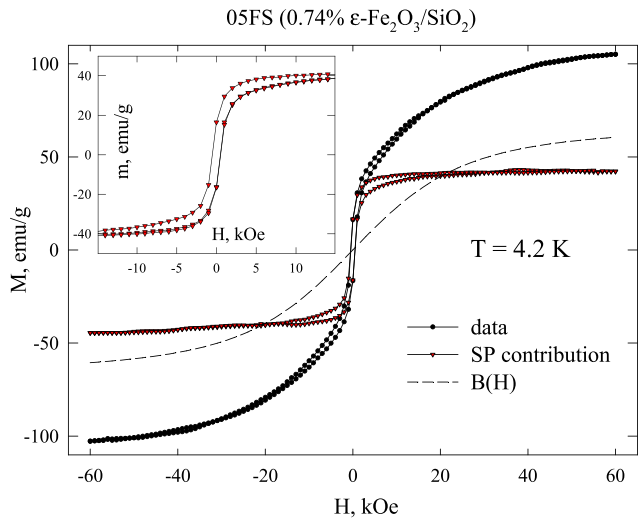

FIG. 4. Field dependence of the magnetic moment M(H) at T = 4.2 K for the studied sample (circles) and corresponding SP contribution (triangles) after subtraction of the paramagnetic contribution 65 emu/g × B(H, T) (dashed curve). Inset: M(H) hysteresis of the SP contribution in the low-field range.

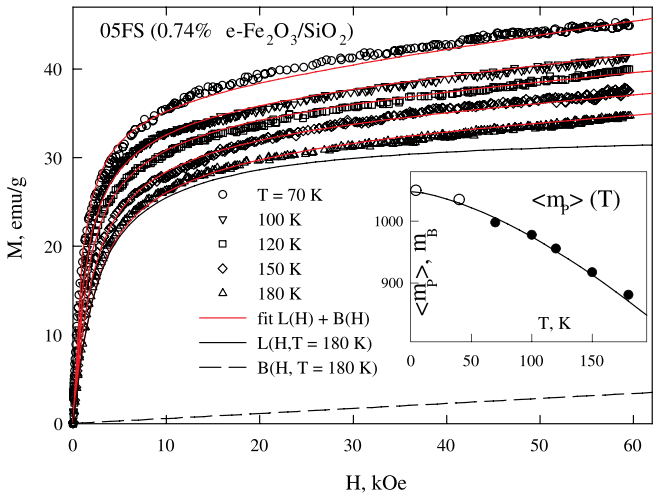

FIG. 5. The experimental M(H) dependences (symbols) of studied sample at different temperatures (given in the figure) and results of the best fit by Eq. (1) (red solid curves). Also shown the SP and paramagnetic contributions (black solid and dashed curves correspondingly) to the fit for T = 180 K. Inset: the temperature variation of mean particle moment ⟨μP⟩(T) (symbols) and the solid curve is the Bloch's $T^{3/2}$ law.

At temperatures above 50 K, the dependences M(H) are fully reversible. Figure 5 presents the isotherms M(H). At temperatures far above T_B, the magnetization curve of SP particles is usually described by the Langevin function $L(x) = \coth(x) - 1/x$, where $x = \mu_P$ H/kT and μ_P is the magnetic moment of a particle. In this study, we described the experimental dependences M(H) using the effective size distribution shown in Fig. 1. When μ_P is proportional to the particle volume, the best agreement for different temperatures is reached at the minim set of fitting parameters.

The particle moment μ_P was determined as $\mu_P = N_{Fe} \times \mu_{eff}$, where μ_{eff} is the effective magnetic moment per iron atom in Bohr magnetons. Number N_{Fe} of Fe(III) atoms in a particle was calculated in the cubic shape approximation (for particles less than 3.5 nm, the effective size $d_{eff} = d - 2 \times 0.31$ nm was used for this calculation). Consequently, the dependence M(H) in emu/g is determined as

$$M(H) = N_{para} \times S \times g \times \mu_B \times B(H) + n_P \sum L(\mu_P) \times \mu_P. \quad (1)$$

In this expression, the first term corresponds to the paramagnetic contribution discussed above, N_{para} is the number of "paramagnetic" atoms Fe(III) per gram of Fe_2O_3 (i.e., the number of shell atoms for d less than 3.5 nm; $N_{para} \approx 1.4 \times 10^{21}\ g^{-1}$), and the product $N_{para} \times S \times g \times \mu_B$ equals to ≈65 emu/g for S = 5/2, g = 2. The second term of expression (1) corresponds to SP contribution, where summation is made over all the particles fixed in the HRTEM measurements (the data in Fig. 1 were obtained for $n_{HRTEM} = 259$ particles); and number n_P is obviously coming from full amount of particles n per gram of Fe_2O_3, i.e., $n = n_P \times n_{HRTEM}$. Again, n_P is determined by the ratio between the number of iron atoms per unit Fe_2O_3 mass ($N = 7.5 \times 10^{21}\ g^{-1}$) to the number of iron atoms N_{HRTEM} in the sampling fixed by HRTEM: $n_P = N/N_{HRTEM}$. For the HRTEM data, one obtain $N_{HRTEM} \sim 4.4 \times 10^5$ iron atoms in $n_{HRTEM} = 259$ particles, and n_P equals to $\approx 1.7 \times 10^{16}$. The agreement of experimental data and fitting by expression (1) was reached at the value $n_P \approx 1.56 \times 10^{16}$, which amounts to 92% of the calculated value $\approx 1.7 \times 10^{16}$ and is in good quantitative agreement for the system of nanoparticles of extremely small size. In the fitting at different temperatures, the only parameter, μ_{eff} determining the value of μ_P, was changed. Solid lines in Fig. 5 show the fitting results. The temperature evolution of average magnetic moment $\langle \mu_P \rangle$ of particles ($\langle \mu_P \rangle = (1/n_{HRTEM})\ \Sigma \mu_P$) is illustrated in Fig. 5 by dark symbols (light symbols correspond to the processing of the dependences M(H) at T = 4.2 and 40 K in strong fields (higher than 20 kOe) when there is no hysteresis related to the blocking). It was established that the dependence $\langle \mu_P \rangle(T)$ in the low-temperature region obeys the well-known Bloch law $\langle \mu_P \rangle(T) = 1 - \text{const} \cdot T^{3/2}$, which follows from the consideration of spin waves in ferro- and ferrimagnets.

The value of $\langle \mu_P \rangle$ at T = 0 is $\sim 1050\ \mu_B$; therefore, according to the above-used relation $\mu_P = N_{Fe} \times \mu_{eff}$, μ_{eff} at T = 0 is $\sim 0.76\ \mu_B$ per Fe(III) atom. This exceeds by far the magnetostatic measurement and neutron diffraction data[16–19] for the ε-Fe_2O_3 particles 25–100 nm in size. We may conclude that in the investigated ε-Fe_2O_3 particles with the characteristic size of ~3 nm, the effective moment per iron atom grows. Based on the reported values $\mu_{eff} \approx 0.3\ \mu_B$ for ε-Fe_2O_3, we obtain that the additional moment of small particles can be caused by the ferromagnetic ordering of magnetic moments of approximately one eighth of iron atoms in a particle if each of these atoms yields 5 μ_B. Indeed, according to one of the Neel hypothesis,[33] the small antiferromagnetic particle can have a magnetic moment because of the odd number of planes and, in the simplest case of two sublattices, the magnetic moment is proportional to the number of magnetically active atoms in the power of 2/3. For ε-Fe_2O_3, the situation is more complex, since iron atoms are in four nonequivalent positions; it is quite probable, however that due to smallness of the particle size, there are uncompensated planes with the ferromagnetic ordering in the particles. The resulting magnetic moment of a particle, which causes the SP behavior, is formed from the ferrimagnetic ordering, presumably in the particle core, and the addition moment form an uncompensated plane.

The magnetic moment measurements in the field H = 1 kOe at temperatures up to 950 K (left panel in Fig. 6) showed that the magnetic order in the particles remains up to the temperatures (~850 K) much higher than the magnetic ordering temperatures (510–585 K) reported for ε-Fe_2O_3 by other authors. As was mentioned in Ref. 29, the nonmonotonic behavior of the dependence M(T) at high temperatures (Fig. 6) cannot be related to a foreign phase, e.g., hematite, in the sample. The X-ray analysis of sample 3FS showed no impurities of other iron oxide polymorphs, except for ε-Fe_2O_3. In addition, the static magnetization data are confirmed by the ESR results. The inset in Fig. 6 shows typical ESR spectra for sample 05FS. One can see the resonance absorption in the region g = 2.0 with the characteristic form of the narrow-width line. As the temperature is increased, the absorption line narrows, which indicates the presence of SP nanoparticles in the sample. According to the ESR data, the resonance absorption remains up to ~800 K (Fig. 6); i.e., at these temperatures, the magnetic order remains in the ε-Fe_2O_3 particles.

On the other hand, in study[3] the anomalous behavior of the dependence M(T) of hematite nanoparticles in the range of 700–900 K was described, attributed by the authors to the reduction of Fe_2O_3 oxide nanoparticles to Fe_3O_4 ones in vacuum. In this study, we purposefully investigated sample 05FS by the ESR method in vacuum, analogously to the M(T) measurements, at temperatures up to 800 K. We found that the temperature dependence of the integral intensity of the ESR spectrum is invariable, within the measurement error, at temperature cycling; i.e., no irreversible changes in the magnetically ordered phase occur.

Thus, based on the X-ray, ESR, Mössbauer, and HRTEM data for sample 05FS, we may state that a decrease in the iron content in the sample does not lead to the qualitative changes in the properties of the system or the formation of other polymorphic modification of iron oxide.

As is known, different temperature dependences of sublattice magnetizations in multi-sublattice systems can lead to the occurrence of a compensation point in the dependence

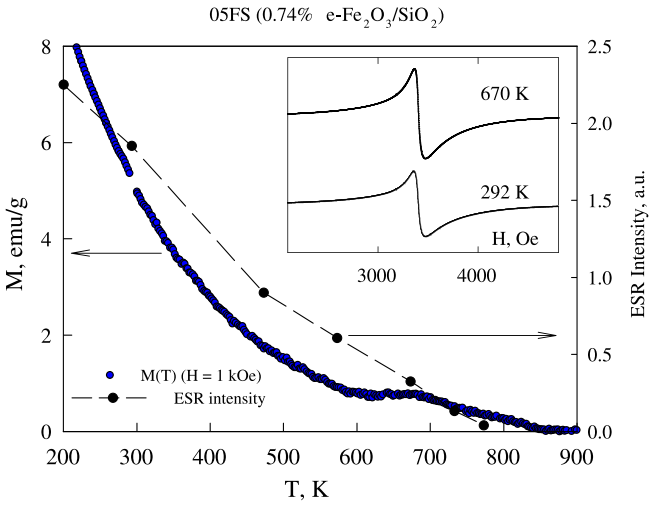

FIG. 6. The temperature dependences of magnetic moment M(T) in field H = 1 kOe (left scale) and integral intensity of the ESR spectrum (right scale) of 05FS sample in the range up to 900 K. Inset: typical ESR spectra of 05FS sample obtained at different temperatures.

M(T).[34] In the author's opinion, the observed nonmonotonic behavior of the dependence M(T) of the investigated particles (Fig. 6) is caused by the contribution of uncompensated sublattices in small ε-Fe_2O_3 particles. This is consistent with the established fact that the magnetic moment of these particles exceeds by far than expected for the ferrimagnetic ordering in larger ε-Fe_2O_3 particles. In other words, both the growth of the magnetic moment of small particles and conservation of the magnetic order along with the nonmonotonic behavior of magnetization above 600 K can be caused by the effect of uncompensated sublattices.

IV. CONCLUSIONS

The magnetic properties of ε-Fe_2O_3 nanoparticles with an average size of ~3 nm were investigated. The magnetic properties of such ε-Fe_2O_3 particles strongly differ from those of the previously studied particles 25–100 nm in size. In the superparamagnetic state caused by the small particle size, no large room-temperature coercivity is observed in the static magnetization curves. The existence of a paramagnetic shell in the particles smaller than ~3.5 nm causes an additional decrease in the effective size of a magnetically ordered particle. However, the value of the specific (bulk) magnetization of ε-Fe_2O_3 particles in the investigated systems of superparamagnetic particles appeared considerably higher than that for the 25–100-nm particles, which was attributed to the effect of uncompensated planes of ferrimagnetically ordered particles with such a small size. This manifests itself in the nonmonotonic behavior of magnetization at high temperatures and conservation of the magnetic order in particles up to ~800 K.

ACKNOWLEDGMENTS

This work was supported by Program of RAS No. 24.40. and by the interdisciplinary project of the Siberian Branch of the Russian Academy of Science No. 45.

[1]S. Mørup, D. E. Madsen, C. Frandsen, C. R. H. Bahl, and M. F. Hansen, J. Phys.: Condens. Matter **19**, 213202 (2007).
[2]T. Ambrose and C. L. Chien, Phys. Rev. Lett. **76**(10), 1743 (1996).
[3]J. Wang, W. Wu, F. Zhao, and G. Zhao, J. Appl. Phys. **109**, 056101 (2011).
[4]Y. A. Kumzerov, N. F. Kartenko, L. S. Parfen'eva, I. A. Smirnov, A. A. Sysoeva, H. Misiorek, and A. Jezowski, Phys. Solid State **54**(5), 1066–1069 (2012).
[5]X. G. Zheng, C. N. Xu, K. Nishikubo, K. Nishiyama, W. Higemoto, W. J. Moon, E. Tanaka, and E. S. Otabe, Phys. Rev. B **72**, 014464 (2005).
[6]I. V. Golosovsky, I. Mirebeau, G. Andre, D. A. Kurdyukov, Y. A. Kumzerov, and S. B. Vakhrushev, Phys. Rev. Lett. **86**, 5783 (2001).
[7]I. V. Golosovsky, I. Mirebeau, D. A. Kurdyukov, and Y. A. Kumzerov, Phys. Rev. B **72**, 144409 (2005).
[8]F. Bødker, M. F. Hansen, C. B. Koch, K. Lefmann, and S. Mørup, Phys. Rev. B **61**, 6826 (2000).
[9]R. D. Zysler, M. V. Mansilla, and D. Fiorani, Eur. Phys. J. B **41**, 171 (2004).
[10]Y. A. Koksharov, S. P. Gubin, I. D. Kosobudsky, G. Y. Yurkov, D. A. Pankratov, L. A. Ponomarenko, M. G. Mikheev, M. Beltran, Y. Khodorkovsky, and A. M. Tishin, Phys. Rev. B **63**, 012407 (2000).
[11]K. Nadeem, H. Krenn, T. Traussnig, R. Würschum, D. V. Szabo, and I. Letofsky-Papst, J. Appl. Phys. **111**, 113911 (2012).
[12]R. D. Desautels, E. Skoropata, Y.-Y. Chen, H. Ouyang, J. W. Freeland, and J. van Lierop, J. Phys.: Condens. Matter **24**, 146001 (2012).
[13]R. H. Kodama and A. E. Berkowitz, Phys. Rev. B **59**, 6321 (1999).
[14]E. Tronc, C. Chaneac, and J. P. Jolivet, J. Solid State Chem. **139**(1), 93–104 (1998).
[15]L. Machala, J. Tucek, and R. Zboril, Chem. Mater. **23**, 3255 (2011).
[16]E. Tronc, C. Chaneac, J. P. Jolivet, and J. M. Greneche, J. Appl. Phys. **98**, 053901 (2005).
[17]S. Ohkoshi, S. Sakurai, J. Jin, and K. Hashimoto, J. Appl. Phys. **97**, 10K312 (2005).
[18]S. Sakurai, J. Jin, K. Hashimoto, and S. Ohkoshi, J. Phys. Soc. Jpn. **74**(7), 1946–1949 (2005).
[19]M. Gich, A. Roig, C. Frontera, E. Molins, J. Sort, M. Popovici, G. Chouteau, D. Martín y Marero, and J. Nogues, J. Appl. Phys. **98**(4), 044307 (2005).
[20]M. Popovici, M. Gich, D. Niansk, A. Roig, C. Savii, L. Casas, E. Molins, K. Zaveta, C. Enache, J. Sort, S. de Brion, G. Chouteau, and J. Nogus, Chem. Mater. **16**(25), 5542 (2004).
[21]M. Kurmoo, J.-L. Rehspringer, A. Hutlova, C. D'Orlans, S. Vilminot, C. Estournes, and D. Niznansky, Chem. Mater. **17**, 1106 (2005).
[22]S. Sakurai, S. Kuroki, H. Tokoro, K. Hashimoto, and S. Ohkoshi, Adv. Funct. Mater. **17**, 2278 (2007).
[23]M. Gich, C. Frontera, A. Roig, E. Taboada, E. Molins, H. R. Rechenberg, J. D. Ardisson, W. A. A. Macedo, C. Ritter, V. Hardy, J. Sort, V. Skumryev, and J. Nogues, Chem. Mater. **18**, 3889 (2006).
[24]Y. C. Tseng, N. M. Souza-Neto, D. Haskel, M. Gich, C. Frontera, A. Roig, M. van Veenendaal, and J. Nogues, Phys. Rev. B **79**(9), 094404 (2009).
[25]K. Yamada, H. Tokoro, M. Yoshikiyo, T. Yorinaga, A. Namai, and S. Ohkoshi, J. Appl. Phys. **111**, 07B506 (2012).
[26]A. Namai, S. Sakurai, M. Nakajima, T. Suemoto, K. Matsumoto, M. Goto, S. Sasaki, and S. Ohkoshi, J. Am. Chem. Soc. **131**, 1170 (2009).
[27]S. Sakurai, A. Namai, K. Hashimoto, and S. Ohkoshi, J. Am. Chem. Soc. **131**(51), 18299 (2009).
[28]G. A. Bukhtiyarova, O. N. Mart'yanov, S. S. Yakushkin, M. A. Shuvaeva, and O. A. Bayukov, Phys. Solid State **52**, 826 (2010).
[29]G. A. Bukhtiyarova, M. A. Shuvaeva, O. A. Bayukov, S. S. Yakushkin, and O. N. Martyanov, J. Nanopart. Res. **13**(10), 5527–5534 (2011).
[30]S. S. Yakushkin, A. A. Dubrovskiy, D. A. Balaev, K. A. Shaykhutdinov, G. A. Bukhtiyarova, and O. N. Martyanov, J. Appl. Phys. **111**(4), 044312 (2012).
[31]A. Cabot, P. Alivisatos, W. F. Puntes, L. Balcells, Ò. Iglesias, and A. Labarta, Phys. Rev. B **79**, 094419 (2009).
[32]E. Winkler, R. D. Zysler, and D. Fiorani, Phys. Rev. B **70**, 174406 (2004).
[33]L. Néel, C.R. Acad. Sci. Paris **252**, 4075 (1961).
[34]J. B. Goodenough, *Magnetism and the Chemical Bond* (Interscience publishers, 1963).